AI-Driven CFRP Structure Evaluation: Deep Learning-Powered Automated Air-Coupled Ultrasonic Detection of Defect

Amitabha Datta[1], Sukeerti Kota[2], Srinivasa V[3] & Ramesh Kumar M[4]

Advanced Composites Division
CSIR-National Aerospace Laboratories, Kodihalli, Bengaluru, Karnataka
[a]*Email: amitabha@nal.res.in*

Abstract

In this study, the successful experiments with air-coupled ultrasonic testing (ACUT) conducted on a 300 mm x 300 mm CFRP laminate, constructed from unidirectional Carbon Fibres, has been designed to simulate various types of damage during manufacturing, were presented as part of the experimental data. It was noted that the ACUT results exhibited strong correlations with the ground truth. To improve automated defect detection, a two-stage process was introduced. In the initial stage, C-Scan data acquired from the ACUT system was utilized. This data underwent meticulous analysis by a Convolutional Neural Network (CNN) image classifier, which categorized the images into two primary classes: defects and non-defects. Subsequently, defect instances underwent in-depth processing using Mask R-CNN, a technique that generated bounding boxes and segmentation masks for each defect zone within the images. The entire process was executed utilizing TensorFlow. The ultimate objective of this approach was to provide inspectors with the requisite tools to promptly and accurately discern and assess defects in composite materials, with the potential to substantially enhance the efficiency and precision of quality control processes in composite structures.

Keywords: *Ultrasonic-Testing, Defect identification, Carbon Fiber Reinforced Polymers, Convolutional neural networks*

1 INTRODUCTION

Composites, both in a broader context and with a specific focus on Carbon Fibre Reinforced Polymers (CFRP), have become critical needs across a range of applications, notably in aerospace and automotive industries. This popularity is attributable to their outstanding mechanical attributes, including their lightweight nature, high specific strength, and suitability for tailored designs [1-3]. Ultrasonic Testing (UT), Radiographic Testing (RT), Thermographic Testing, Shearography, and Acoustic Emission (AE) Testing are well-established non-destructive inspection methods for composite structures. UT employs high-frequency sound waves for defect detection and characterization [3-4], RT uses X-rays or gamma rays to reveal internal anomalies [5-6], Thermographic Testing relies on thermal imaging to identify defects [7-8], Shearography measures surface deformation under stress [9-10], and AE Testing monitors acoustic signals during material deformation or failure [11-12]. The choice of method depends on factors such as material properties, defect types, sensitivity requirements, and resource availability. Often, a combination of these techniques is employed to ensure a comprehensive assessment of composite structural integrity. It is important to note that these aforementioned NDT methods represent only a subset of the conventional techniques employed for the assessment of composite structures. The selection of an appropriate method depends on several factors, including the composite material type, the nature of expected defects, required sensitivity, and the availability of necessary resources and equipment. Often, a combination of these methods is employed to ensure a comprehensive evaluation of the structural integrity of the composite structure. The ongoing transition to Industry 4.0 presents new opportunities for advancing inspection procedures through artificial intelligence (AI)-based machine learning and deep learning algorithms, enabling sophisticated data analysis and autonomous systems. Several research groups have used deep learning (DL) algorithms to detect defects in different structures and materials, including A-scan ultrasonic signals, B-scan images, and phased-array ultrasonic images. It is noteworthy that, DL models outperform the traditional methods and even human operators in some cases. Different DL architectures such as Convolutional neural networks (CNNs), Gated recurrent unit (GRU), Scalable and Efficient Object Detection (EfficientDet), and Visual Geometry Group(VGG-16) [21], have been applied to process ultrasonic data, and transfer learning has proven effective in enhancing model performance. These studies collectively suggest that the automation of repetitive NDE tasks is achievable in the medium term, with DL methodologies providing higher accuracy and efficiency than classical approaches.

Guo *et al.* [13] introduced a DL model that combines GRU and CNN architectures to process ultrasonic signals, achieving superior accuracy compared to other networks. Yan *et al.* [14] applied a CNN-Support Vector Machine(SVM) framework for pipeline girth cracking identification using Electro Magnetic Acoustic Transducer (EMAT) signals, outperforming traditional feature extraction methods. DL has also been employed in the context of ultrasonic B-scans for defect detection. Yuan *et al.* [15] utilized a Feed-forward neural networks (FCNN) framework for train wheel defect identification, achieving a 92% recognition rate. Medak *et al.* [16] proposed an EfficientDet network for automated defect detection from ultrasonic B-scan images, outperforming other DL models. Virkkunen *et al.* [17] compared a CNN model's performance to human operators for phased-array ultrasonic B-scan flaw detection, demonstrating the CNN's superiority. Slonski *et al.* [18] explored the automation of flaw detection in concrete through ultrasonic tomography images using a VGG-16 network, reporting a validation accuracy of 97%. Additionally, Ye *et al.* [19] compiled a comprehensive dataset of ultrasonic wavefield images and benchmarked various well-known DL models, revealing DenseNet as the most accurate. These examples collectively demonstrate that DL methodologies have surpassed classical methods and human operators in NDE tasks, offering potential for automating repetitive inspections in the near future.

A. Croxford *et al.* [20], introduces a framework of automation levels for various non-destructive evaluation (NDE) modalities, with a primary emphasis on ultrasound inspection. The proposed levels, depicted in Fig.1, span from traditional NDE procedures where human operators are fully responsible to a future scenario of complete NDE automation without human intervention. Levels 3 and 4 represent fully automated NDE, feeding directly into structural integrity decision-making, enabling data-driven approaches for decisions like acceptance, rejection, maintenance, repair, and remaining useful life estimation. These proposed levels align with the levels recently published by the European Union Aviation Safety Agency (EASA) and are extended here to address a broader range of ultrasonic NDE applications. The transition to higher automation levels is greatly facilitated by the adoption of Deep Learning (DL) methods, enabling more sophisticated automation in handling complex scenarios with minimal operator involvement and the potential for human-free decision-making. However, the need for substantial labelled datasets presents a challenge, which can be mitigated by employing rudimentary DL systems to coarsely label data.

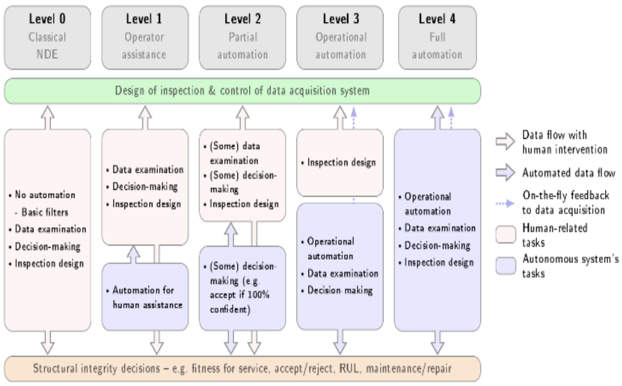

***Fig.1**: Schematic representation of the proposed level of automation by A. Croxford et al.[20]*

At CSIR-NAL, the pursuit of automated ultrasonic inspection is a primary objective. To initiate this automation, as suggested by A. Croxford *et al.*, the air-coupled ultrasonic testing (ACUT) experiments were conducted on a 300 mm x 300 mm CFRP laminate to generate database. In order to improve the process of automated defect detection, a two-stage strategy was implemented. In the first stage, a Convolutional Neural Network (CNN) image classifier use to categorize images into two primary classes: defects and non-defects. Subsequently, further refinement was achieved by subjecting defect instances to comprehensive processing using Mask

R-CNN, a technique for generating bounding boxes and segmentation masks delineating each defect zone within the images. The entire workflow was carried out with the aid of TensorFlow-2.20 and NVIDIA CUDA Cores:10752. The overarching aim of this methodology was to furnish inspectors with the requisite tools for the rapid and precise identification and evaluation of defects present in composite structure.

The organization of the paper is as follows: sec.2 describes the experimental setup and specimen under test; sec.3 describes model development. In sec.4, discuss results, by conclusion in sec.5.

2 EXPERIMENTAL SETUP & SPECIMEN UNDER TEST

Air-coupled ultrasonic testing has demonstrated its high reliability as a technique for inspecting defects in contemporary multilayer composites, encompassing assessments of delamination, air inclusions, bonding quality, and impact-induced damage.

The Air-coupled system developed by The Ultran Group represents a precise system for damage detection in a wide range of materials across various industries illustrated in Fig.2. It includes a fully configured ultrasonic analysis system suitable for both internal and surface imaging, enabling the investigation of defects, heterogeneity, delamination, porosity, velocity/density, thickness, and Time of Flight. The system supports ULTRAN's proprietary scanning package for 2D C-Scan imaging, SecondWave^{TM} Studio software for A-scan point measurements, Line-Scan, and FFT analysis, as well as SecondWave^{TM} Research Studio software for post-processing and statistical evaluation of C-Scan images.

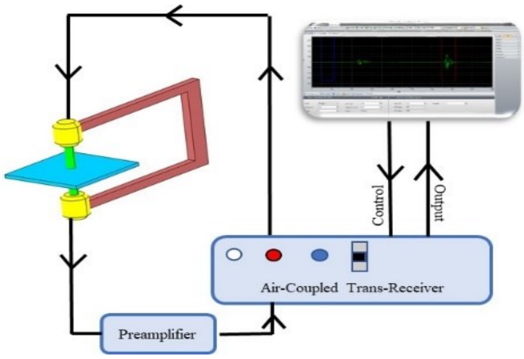

(a)

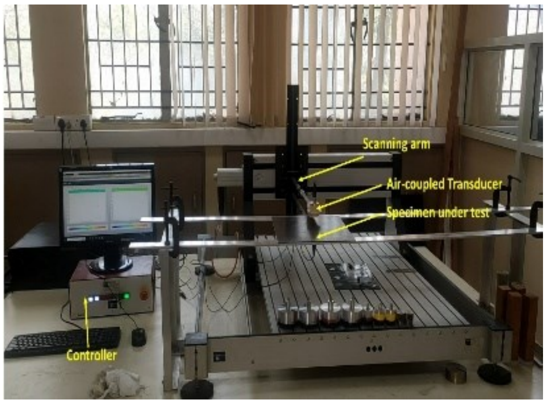

(b)

Fig.2: *(a) Air-Coupled ultrasonic system, comprising a controller, a scanning area, and holders for transducers (b) Picture depicting the system at CSIR-NAL*

A 300mm x 300mm laminate, fabricated from unidirectional Carbon Fibres, has been designed to simulate various types of damages that can occur in composite laminates during manufacturing, as illustrated in Fig.3a. The figure indicates specific insert damages: "1" represents a release film with a 20x20 mm insert, "2" signifies a 20x20 mm UD prepreg backup film insert, "3" denotes a 20x20 mm UD prepreg backup paper insert, "4" corresponds to a 20x20 mm tool tech insert, and "5" indicates a 50x30 mm delamination area within the laminate. The ACUT system combines two point-focused piezoelectric transducers, each with a 38 mm focal length and a valid inspection region with a 13 mm radius. This transducer arrangement facilitates the transmission of bulk waves within CFRP specimens. The ultrasonic signals, generated at a frequency of 140 kHz, are transmitted with a controlled transitional velocity of 10 mm/s in both the horizontal (V_x) and vertical (V_y) directions. The scanning process utilizes a step size of 0.1 mm, ensuring precise coverage of the specimen. Moreover, the system features a gain setting of 70 dB, resulting in enhanced signal sensitivity and detection capabilities. Raw C-Scan image obtained from the system is illustrated in Fig.3b.

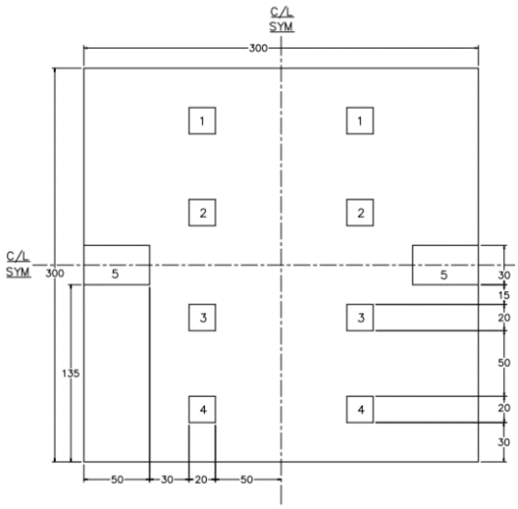

(a)

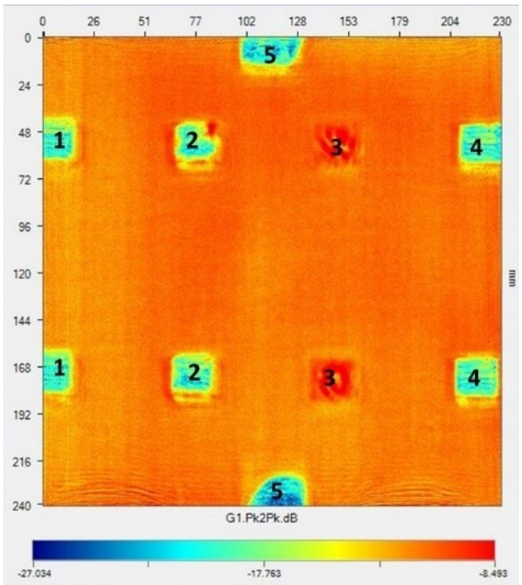

(b)

Fig. 3: *(a) Laminate Design and Damage Simulation: A 300 mm x 300 mm unidirectional CFRP laminate designed to simulate various manufacturing-induced damages within composite laminates (b) Unprocessed C-Scan image rotated 90° Anti-Clockwise relative to Fig. 3a*

2.1 Data Set Generation

In accordance with the procedures detailed in the experimental setup section, we conducted data acquisition by systematically varying parameters including pulse repetition frequency (PRF), transmitter voltage (V), Low-Pass Filter (LPF) and High-Pass Filter (HPF) settings, and adjusting the receiver gain of the ACUT system. This process yielded a total of 63 images. Subsequently, we employed data augmentation techniques, such as image rotation at various angles, flipping, scaling, cropping, brightness enhancement, contrast adjustment, and the adding white noise to the images. These augmentation methods allowed us to expand our dataset to a total of 321 images for further analysis and experimentation.

3 MODEL DEVELOPMENT

As outlined in sec. 1, our objective was to develop an algorithm for shape detection and damage size estimation within the test specimen. To achieve this, we adopted a two-stage approach, as illustrated in Fig.4. In the first stage, as indicated in the flowchart, we performed CNN based classification on the C-scan image of the test panel. Subsequently, at stage-2, in cases where damage was detected, we utilized Mask-RCNN on the C-scan images to identify arbitrary shapes and calculate the extent of the damage.

The raw C-scan image, initially sized at [1000, 600], was subjected to de-noising (optional) and evaluated by a CNN-based classifier to ascertain the presence or absence of damage in the input image. We opted for a CNN-based Classifier due to its proven ability to accurately recognize damage in images, its capacity to autonomously learn and extract intricate features, and map them to their respective classes, ensuring precise image classification. Furthermore, CNNs exhibit adaptability to diverse damage sizes, scales, and orientations.

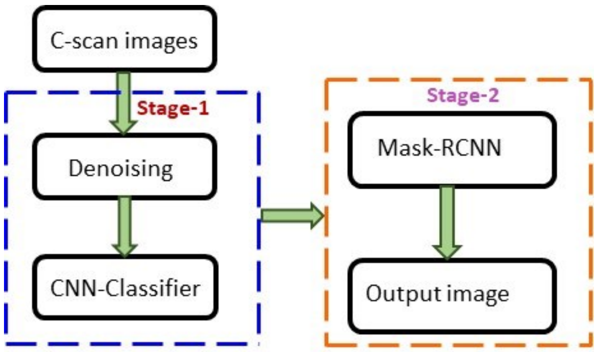

Fig.4: *Flowchart representation of the Model: Classifying C-scan images in the first stage and, when damage is detected, using Mask R-CNN to identify shapes and measure the damage's extent in the second stage*

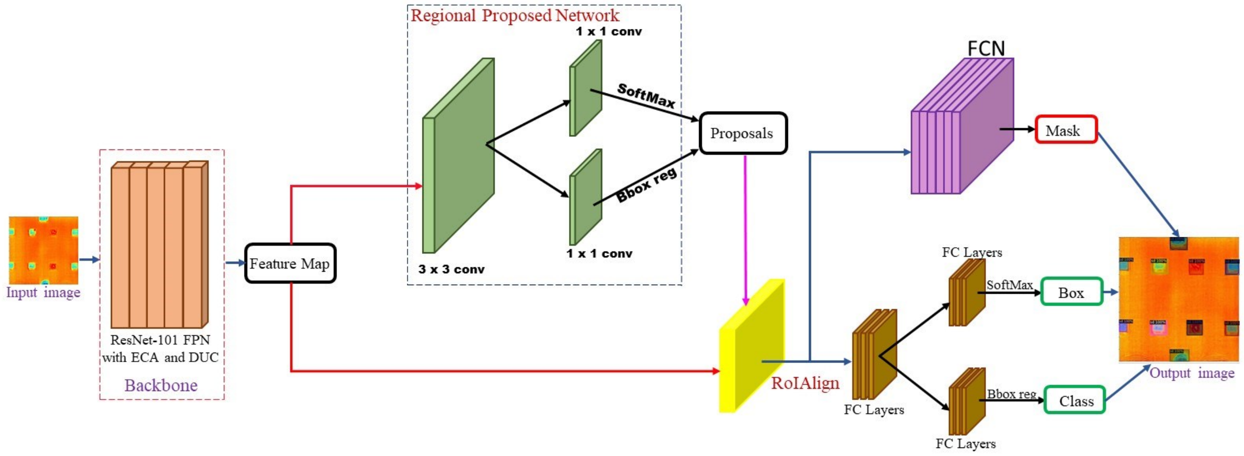

Fig. 5: *Mask R-CNN architecture for defect zone bounding boxes and segmentation masks*

After damage has been classified, the input image is first passed through a backbone network, which is typically a deep convolutional neural network (CNN) like ResNet-101 and Feature Pyramid Network (FPN) architecture. The backbone network extracts a set of feature maps at different scales, representing features from low-level edges and textures to high-level object and context information as illustrated in Fig.5.

By applying ResNet-101 to our data set, the method gives Pool size as 7, Maximum pool size as 16, Mask shape [28, 28], ROI positive ratio 0.33. The weights of each feature have been calculated based on minimum values, maximum values, and standard deviation of the objects.

In the image processing pipeline, the first step involves calculating the number of pixels and their intensity in the input image, using a utility function that extracts information from a NumPy array to obtain details about bounding boxes, including shapes, minimum, and maximum values. The kernel function used for processing is a [3x3] filter, and the image is compressed to a 0-255 scale.

For segmentation, the input image is passed through a Region Proposal Network (RPN), it plays a critical role in identifying potential defect recognition, improving the overall efficiency and accuracy of the Mask R-CNN model in image segmentation tasks. It achieves this by sliding set of anchor boxes of different scales and aspect ratios across the feature map produced by a backbone Network. The RPN then predicts the likelihood of each anchor box containing an object and refines their positions with multiple bounding boxes regression.

After defining the regions, the output of the RPN and feature maps from RES-NET101 and Feature Pyramid Network (FPN) will be the input of the is RoI Alignment or RoI Pooling techniques which is a Pooling layer, where the size of the proposed regions can be determined.

Features obtained from RoI alignment are set for the model and passed through Fully Connected Layers (FCL) and Fully Connected Network (FCN). This step aids in visualizing how to design and generate masks over an image.

The model is pre-trained on the COCO dataset [21], which consists of over 330,000 images, each annotated with 80 object categories and 5 captions describing the scene. Weights for each feature are calculated based on minimum values, maximum values, and the standard deviation of objects.

We have presented one of the sample C-Scan image of our data set from stage -1 to stage-2 in Sec.4

4 RESULTS

In this study, we present two key outcomes. First, we describe the outcome of the classification process conducted using a CNN-Classifier implemented through Keras illustrated in Fig.6a. Subsequently, performance of the Mask R-CNN algorithm illustrated in Fig. 6b, which was initially trained to detect various defects and shapes based on specific detection requirements. The model demonstrated satisfactory performance across most detection tasks.

Pre-trained weights are available for the Mask R-CNN model and can be utilized for defect detection, with the option to update these weights during subsequent model training.

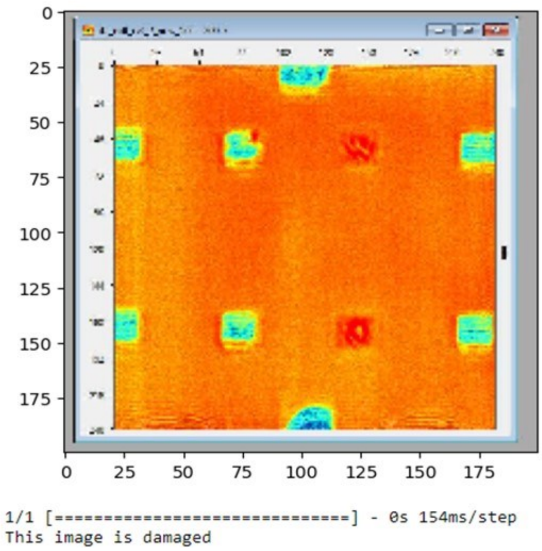

(a)

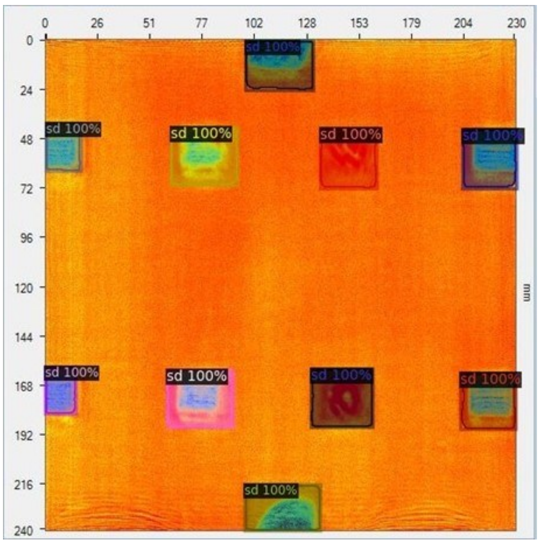

(b)

Fig.6: *(a) CNN Image classifier: Whether the image is damage or not (b) Mask R-CNN: Creates a mask over the damage area*

To refine the model's ability to identify objects and shapes, we conducted further training using our dataset that included various shapes. The model underwent training and validation testing, achieving a mean Average Precision (mAP) of 89% after 1000 epochs. The validation loss function plateaued at 0.004, while accuracy consistently remained around 0.988 for our dataset. These findings demonstrate the model's capacity to effectively detect both small, clustered objects within a single image and larger or medium-sized objects in an image.

5 CONCLUSION

Ultrasonic testing (UT) is one of the most widely used non-destructive inspection methods for inspection of composite structure. The artificial intelligence (AI) based machine learning and deep learning algorithm play a critical role in facilitating the advancement of automated inspection procedures for UT data. In this context, air-coupled ultrasonic testing (ACUT), we have successfully conducted experimental using composites panels with and without defect. ACUT results shows good correlation with ground. To facilitate automated defect detection, our algorithm employs a two-stage process. In the initial stage, we utilize C-Scan data generated by the ACUT system and analysed through a Convolutional Neural Network (CNN) image classifier, responsible for classifying the images into two categories: defects and non-defects. Subsequently, the defect instances are processed using Mask R-CNN, which generates bounding boxes and segmentation masks for each defect zone within the image with mPA of 89%. This process is implemented using TensorFlow. The the model's accuracy can increase further, by adjusting the hyperparameters, which can encompass aspects like kernel types, regularization strengths, or learning rates.

ACKNOWLEDGMENT:
Authors express their since thanks to Director, CSIR- NAL for his encouragement and support.

6 REFERENCES

[1]. Degenhardt, Richard *et al.* "Future structural stability design for composite space and airframe structures", Thin-Walled Structures 81 (2014): 29-38.

[2]. M.O.W. Richardson and M.J. Wisheart, "Review of low-velocity impact properties of composite materials", Composites Part A: Applied Science and Manufacturing, Vol. 27, Issue 12 (1996).

[3]. Cheng, Xiaoying, *et al.,* "Automatic defect depth estimation for ultrasonic testing in carbon fiber reinforced composites using deep learning", NDT & E International 135 (2023): 102804.

[4]. Silva, Maria Inês *et al.,* "Review of conventional and advanced non-destructive testing techniques for detection and characterization of small-scale defects", Progress in Materials Science (2023): 101155.

[5]. Pannier, Yannick *et al.,* "Automatic segmentation and fibre orientation estimation from low resolution X-ray computed tomography images of 3D woven composites", Composite Structures 318 (2023): 117087.

[6]. Guo, Rui *et al.,* "Deep-learning image enhancement and fibre segmentation from time-resolved computed tomography of fibre-reinforced composites", Composites Science and Technology 244 (2023): 110278.

[7]. Lecompagnon, Julien *et al.,* "Non-destructive thermographic detection of internal defects using pixel-pattern based laser excitation and photothermal super resolution reconstruction", Scientific Reports 13.1 (2023): 3416.

[8]. Daghigh, Vahid, and Mohammad Naraghi, "Machine learning-based defect characterization in anisotropic materials with IR-thermography synthetic data", Composites Science and Technology 233 (2023): 109882.

[9]. Hung, Y. Y., and H. P. Ho, "Shearography: An optical measurement technique and applications", Materials science and engineering: R: Reports 49.3 (2005): 61-87.

[10]. Hung, Michael YY, HuaiMin Shang, and Lianxiang Yang, "Unified approach for holography and shearography in surface deformation measurement and non-destructive testing", Optical engineering 42.5 (2003): 1197-1207.

[11]. Yu, Yeun-Ho, *et al.*, "A study on the failure detection of composite materials using an acoustic emission", Composite structures 75.1-4 (2006): 163-169.

[12]. Kordatos, E. Z., D. G. Aggelis, and T. E. Matikas, "Monitoring mechanical damage in structural materials using complimentary NDE techniques based on thermography and acoustic emission", Composites Part B: Engineering 43.6 (2012): 2676-2686.

[13]. Y. Guo, Z. Xiao, L. Geng, J. Wu, F. Zhang, Y. Liu, W. Wang, "Fully convolutional neural network with GRU for 3D braided composite material flaw detection", IEEE Access 7 (2019) 151180–151188.

[14]. Y. Yan, D. Liu, B. Gao, G. Tian, Z. Cai, "A deep learning-based ultrasonic pattern recognition method for inspecting girth weld cracking of gas pipeline", IEEE Sensors Journal 20 (2020) 7997–8006.

[15]. M. Yuan, J. Li, Y. Liu, X. Gao, "Automatic recognition and positioning of wheel defects in ultrasonic B-Scan image using artificial neural network and image processing", Journal of Testing and Evaluation 48 (2019) 308–322.

[16]. D. Medak, L. Posilović, M. Subašić, M. Budimir, S. Lončarić, "Automated defect detection from ultrasonic images using deep learning", IEEE Transactions on Ultrasonics, Ferroelectrics, and Frequency Control (2021).

[17]. I. Virkkunen, T. Koskinen, O. Jessen-Juhler, J. Rinta-Aho, "Augmented ultrasonic data for machine learning", Journal of Non-destructive Evaluation 40 (2021) 1–11.

[18]. M. Słoński, K. Schabowicz, E. Krawczyk, "Detection of flaws in concrete using ultrasonic tomography and convolutional neural networks", Materials 13 (2020) 1557.

[19]. J. Ye, N. Toyama, Benchmarking deep learning models for automatic ultrasonic imaging inspection, IEEE Access 9 (2021) 36986–36994.

[20]. Cantero-Chinchilla, Sergio, Paul D. Wilcox, and Anthony J. Croxford, "Deep learning in automated ultrasonic NDE–developments, axioms and opportunities", NDT & E International (2022): 102703.

[21]. Tsung-Yi Lin, Maire, M., Belongie, S. J., Bourdev, L. D., Girshick, R. B., Hays, J., … Zitnick, C. L. (2014). Microsoft COCO: Common Objects in Context. CoRR, abs/1405.0312. Retrieved from http://arxiv.org/abs/1405.0312.